Journal of Thermal Analysis and Calorimetry, Vol. 91 (2008) 3, 817–823

CHARACTERIZATION OF EXFOLIATED GRAPHITE FOR HEAVY OIL SORPTION

Gabriela Hristea and P. Budrugeac*

Non-Conventional Engineering Department, National Research Institute for Electrical Engineering – Advanced Research, INCDIE ICPE-CA, Splaiul Unirii 313, 030138, Bucharest, Romania

In this paper are reported some experimental data related to the influence of preparation regimes and characteristics of exfoliated graphite based sorbents produced by thermal expansion of H_2SO_4-graphite intercalation compounds (H_2SO_4–GICs) on their sorption properties. Investigations involving X-ray diffraction analyses, surface area, bulk density and oil sorption capacity measurements, have been performed. Sorption capacity was discussed as a function of bulk density, total pore volume and surface area. Some empirical correlation between studied characteristics of exfoliated graphite have been found. The differences among the obtained samples, as a consequence of synthesis conditions, were also put in evidence by thermal analysis (TG, DTG and DTA) performed after their exposure to oil sorption.

It was found that thermal analysis method could provide information about the exfoliated graphite pore system related to the sorbed oil oxidation rate. The capacity for oil uptake was also discussed in the case of graphite oxide soot.

Keywords: *adsorption, environment, materials, porous media, powders, processing*

Introduction

There is nowadays an increased interest in the thermal characteristics of materials with a micrometric scale [1]. This interest concerns also the use of thermogravimetry to evaluate the reactivity of a wide range of nano/microstructured materials including various forms of carbon materials [2–5]. This paper deal of exfoliated graphite (EG) as a carbon material of growing importance due to its numerous actual and potential applications.

Design and control of carbon materials structure for enhanced performances such as highly efficient sorbents for removal of oil products from water surface is of great environmental importance. EG, due to its peculiar properties proved to be an efficient sorbent for gathering and removal of crude oil from water surface [6–9].

When some graphite intercalation compounds (GICs) are rapidly heated at high temperatures (~1000°C) the intercalated material is decomposed to gaseous compounds and as a consequence, marked exfoliation of the graphite occurs. This exfoliated graphite has wide applications when it is pressed to make thin sheets of graphite. Anyway, different pore sizes in carbon materials are required in their applications [10–14], so that the control of pore structure is one of the important issues being reviewed and discussed in detail [15]. Recently, it was found out that exfoliated graphite is able to sorb a large amount of heavy oil [16]. The same feature of a good oil sorption capacity was found to be provided by the graphite oxide soot [17].

This paper presents some aspects regarding physical characterization of graphite oxide soot and three types of EG as well as the relationship between their properties, as a consequence of preparation regimes. The sorption capacity of expanded samples and thermal analysis performed on those one along with sorbed oil was also discussed. Thermal analysis will be proposed as a method that could provide information about the exfoliated graphite pore system related to sorbed oil oxidation rate.

Experimental

The EG was prepared by thermal exfoliation of different H_2SO_4–GICs. Intercalated compounds were obtained through liquid methods [18], by immersion of natural graphite (400 μm grain size) in acid solutions. Natural graphite produced in China with 98 mass% carbon content was used as host material for intercalation. The structural states of the surface and volume of EG particles can be controlled by means of changing the oxidizing treatment and applied temperature program. With this in view, different oxidizing conditions, consisting in: different

* Author for correspondence: gabrielahristea@yahoo.com

1388–6150/$20.00

Akadémiai Kiadó, Budapest, Hungary
Springer, Dordrecht, The Netherlands

reagents ratio and concentrations, different oxidizing agents, have been experimented. The used compositional variants are presented in Table 1.

Natural graphite is suspended in a mixture of H_2SO_4 and HNO_3. An oxidizing agent such as $KMnO_4$ or $FeCl_3$ was added to the oxidation mixture in small quantities, over a period of a few hours in a cooled flask. The time allotted for reactions was of 2 days. After this period, the resulted products were stirred with distilled water, then settled and decanted until the wash water became neutral. The suspensions are suction – filtered as much as possible, dried in vacuum at 50°C to constant mass.

To achieve exfoliation, the resulting products, obtained according to E1, E2, E3 and E4 processing variants (as presented in Table 1), have been subsequently exposed to a thermal shock at 900°C, in a graduated quartz glass beaker placed in an electrical furnace. After a few seconds the ICs decomposed and instantaneously expanded. After this procedure the expanded volume, V (mL) and net mass W (g) were measured for each compound, to obtain the specific expansion volume per gram graphite V/W (mL g^{-1}). Thus, graphite oxide soot and three types of expanded graphite were obtained. These were marked for recognition after the starting compositional variants, as: E1, E2, E3 and E4.

Bulk density has been determined in accordance with a Romanian Standard No. 8432/79 [19] by measuring the mass M(g) of an expanded sample, resulting by its free falling in a measured volume V (cm^3). The ratio between mass and measured volume, M/V, gives the specimen bulk density.

Surface areas of the expanded species were measured by nitrogen gas adsorption at 77 K in a surface analyzer (Coulter, SA 3100), by applying the Brunauer Emmett–Teller (BET) equation.

The volume of micropores was deduced from N_2 adsorption isotherm at 77 K by applying Dubinin-Radovich equation [20]. The volume of narrow micropores was consequently deduced from CO_2 adsorption isotherm at 273 K.

The structure of graphite oxide (GO) and GICs, before and after thermal processing has been characterized by X-ray diffraction with CuK_α radiation, using HZG4 A2 equipment. The crystallinity of exfoliated samples was estimated by computing the ratio of crystalline peak to entire area for each obtained X-ray pattern presented in Fig. 3 [21].

Heavy oil of 0.88 g cm^{-3} density, produced by Lisiachansk Oil Processing Plant, was used for the sorption experiments, according to the following procedure: heavy oil was added to a weighed sample of expanded graphite sorbent, until saturation was achieved. The unsorbed oil was removed during 12 h using filter paper. The exfoliated graphite sorbent along with the adsorbed oil was weighed and the specific sorption was estimated from the mass increase due to adsorbed oil. It was experimentally shown by other authors [22] that the specific sorption values obtained by this method are in close agreement with those for oil sorption at the water surface.

The structural differences between samples are also reflected by the thermal behavior of the oil-exfoliated samples systems, which have been investigated by thermal analysis methods (TG, DTG, DTA). The simultaneous recording of TG, DTA and DTG curves was performed using a Q-1500D Paulik–Paulik–Erdey derivatograph (MOM-Budapest). Applied non-isothermal recording conditions were: static air atmosphere, temperature range 20–500°C, heating rate of 2.5 K min^{-1}, opened sample pans.

Results and discussions

Characterization of synthesized EG

Table 1 shows the experimental conditions for GO and ICs synthesis and some of their physical characteristics

Table 1 Compositional variants /synthesis conditions and characteristics of exfoliated samples

Sample	Synthesis conditions		Characteristics of exfoliated samples				
	Reagents molar ratio, H_2SO_4: HNO_3*	Oxidizing agent, 5%	Bulk density/g cm^{-3}	Specific expansion volume/cm^3 g^{-1}	Surface area, S_{BET}/m^2 g^{-1}	Sorption capacity, C_{sorpt},/ L(100g EG)$^{-1}$	Pore volume mL g^{-1}
E1	9:1	$KMnO_4$	0.0096	40	90.0	0.9	1.44
E2	1:1	$KMnO_4$	0.00394	80	158.0	9.7	2.33
E3	4:1	$KMnO_4$	0.00469	65	116.0	8.33	0.83
E4	9:1	$FeCl_3$	0.02573	25	11.0	2.4	0.29
Pristine graphite (Natural graphite used as raw material)			0.5999	–	1.6	0.1	

*In all variants H_2SO_4: 98% and density: 1.84 g cm^{-3} was used. For E1, E3, E4 variants HNO_3 63%, and density: 1.43 g cm^{-3} was used. For E2 variant HNO_3 30%, d: 1.18 g cm^{-3} was used

obtained after the exfoliation process, respectively: bulk density, specific expansion volume, surface area, oil sorption and pore volume.

Since the exfoliation results from vaporization and decomposition of intercalates, the degree of exfoliation process should be directly related to the amount of intercalates [23]. In present experiments, applying different oxidizing conditions to a natural graphite substrate became obvious that the precursor for thermal exfoliation reaction was different in each case. As it was expected, due to a high degree of graphite oxidation resulted by $KMnO_4$ treatment, were obtained compounds with a specific expansion volume value higher than those obtained by $FeCl_3$ addition (as is shown in Table 1).

Even the specific expansion volume achieved in this case is smaller as compared with that obtained using $KMnO_4$ as oxidant, this procedure proved to be suitable because in this case, reaction is slightly exothermal (mild conditions) and filtration procedure goes easier. Moreover, after exfoliation process, the $FeCl_3$ traces remained on the graphite grains surface which allows that the graphitic substrate to have an increased conductivity, which is adequate for other kinds of practical applications.

According to X-ray diffraction pattern shown in Figs 1 and 2, it should be noticed that for the same 2 days reaction time, in the case of $KMnO_4$ oxidation, different stages of intercalation are achieved. This behavior seems to come from different reagents ratios used in starting compositional variants. Only higher stage graphite salts are formed when the concentration of the sulfuric acid is too low as a consequence of the addition of larger quantities of nitric acid, as is the case of E2 and E3 sample. The formation of graphite oxide need a stage–1 GIC as a precursor (Fig. 1). Clearly the thermal precursor for thermal exfoliation reaction was different with the sample E1 from the other one.

This is also reflected by the physical characteristics of investigated samples (as is shown in Table 1). For E1 sample with H_2SO_4 used in excess, the reaction leads to a graphite oxide type structure [23]. In Fig. 1, the (001) diffraction line of graphite oxide appeared together with the (002) and (004) lines of carbon. During this process, the stacking sequence would vary from A/AB/BA/A…(stage 2 GIC) to A/A/A/A… (stage 1 GIC). Instead, by using a stoechiometric ratio between the reagents of 1:1, a H_2SO_4-GIC with stages 2 and 3 mixture (sample E2) was obtained. In Fig. 3 it is also shown the X-ray diffractogram of natural graphite (pristine graphite) used as raw material for intercalation processes.

By applying the expansion procedure, more or less crystalline structures are obtained. As an

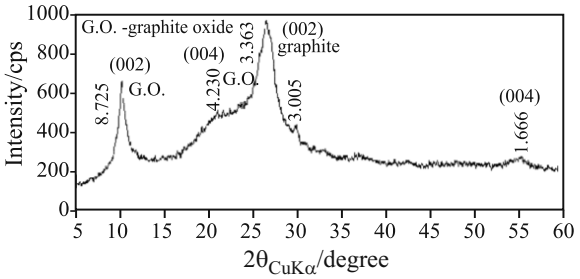

Fig. 1 X-ray diffraction pattern of E1 sample (graphite oxide)

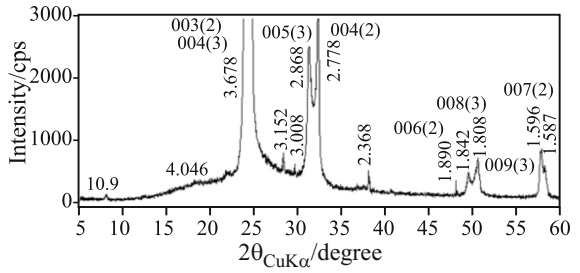

Fig. 2 X-ray diffraction pattern of E2 sample

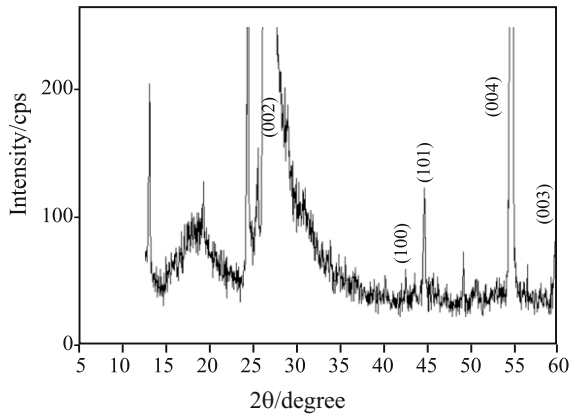

Fig. 3 X-ray diffraction pattern of natural graphite (pristine graphite)

experimental observation, graphite oxide soot and EG species obtained from compositional variants with $KMnO_4$ showed more amorphous structures than EG obtained with $FeCl_3$ which presents a relatively high order degree, as shown in Fig. 4.

The XRD pattern of sample E4 after expansion suggests a strong preferred orientation of the crystallites of the powder, so that the graphitic planes (00l) are oriented parallel to the powder surface. The same effect could be provided by the turbostratic structure of the sample, with no 3D ordering of the graphitic sheets. Assuming that after expansion, E4 is pure graphite, the value of the interlayer distance d(002)=3.39 Å, smaller than the turbostratic limit, 3.44Å, could indicate that there is not a turbostratic structure, which is in agreement with the large crystallite size along the *c* axis; the crystallite size could be deduced from the (002) line width. In addition, some quantitative estimations concerning the

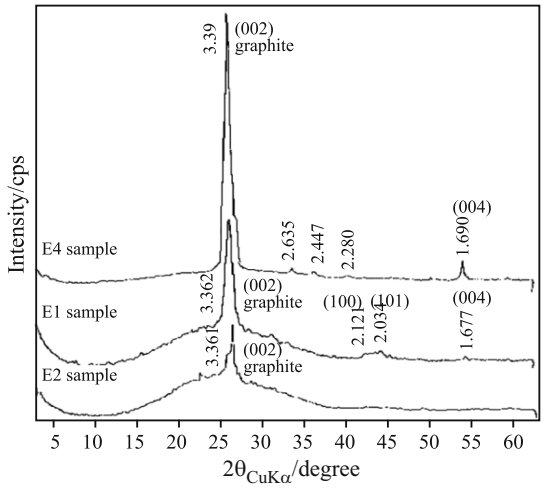

Fig. 4 X-ray diffraction pattern of E1, E2 and E4 samples, after thermal processing at 1000°C

crystallinity of E1, E2 and E4 exfoliated samples have been done, by computing the ratio of crystalline peak related to the entire pattern area of corresponding X-ray pattern showed in Fig. 3. Accordingly, the following crystallinity values were obtained: 16.8% for E1 sample; 7.3% for E2 sample and 36.2% for E4 sample.

Oil sorption

It was found that each EG type and the GO soot could adsorb heavy oil, at room temperature, very quickly, within few seconds. It was also observed that in the case of oil spilt in water, the preferential adsorption of oil and no adsorption of water occurred [24]. Also, natural graphite subjected to oil sorption from water sediments, unlike EG which remained suspended on the water surface. As is shown in Table 1, pristine graphite has a sorption capacity value of 0.1 L/100 g, which is much lower than expanded samples one (2.4–9.7 L/100 g). As it was expected sorption capacity increase with surface area.

Certain dependence between sorption capacity: C_{sorpt} and the above mentioned physical characteristics of the exfoliated specimens have been found. This partly reflects the synthesis conditions and their influence on physical and functional properties.

Figures 5 and 6 show the dependence of the sorption capacity *vs*. the surface area and the bulk density, ρ, respectively. It can be noticed that for all investigated samples the sorption capacity increases linearly with the surface area, in the following order: pristine graphite<E4< E1< E3<E2.

Also, plots of lg C_{sorpt} *vs*. lg ρ showed a linear correlation according to the relationship:

$$\log C_{sorpt}=\text{const.}-n \log \rho$$

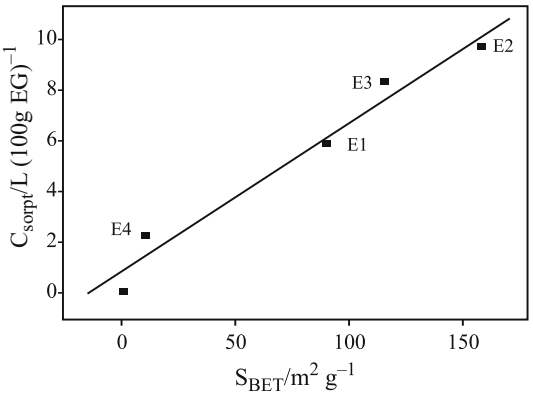

Fig. 5 Oil sorption capacity *vs*. surface area of exfoliated graphite samples

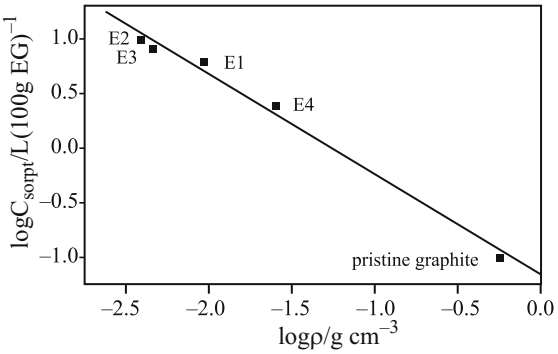

Fig. 6 log C_{sorpt} *vs*. log ρ of exfoliated graphite samples

where n=0.9; the correlation coefficient of the linear regression is 0.996.

The same variation order of sorption capacity increase with bulk density has been noticed, respectively: pristine graphite<E4<E1<E3<E2.

To analyze the obtained results, notions referring to discretion and surface homogeneity should be taken into account. Thus, on the considered carbon surface there are uniformly located several distinct, active sites, where sorption forces can act. In the case of analyzed carbon materials, such kinds of active sites are represented by the pores system. Usually to obtain a solid sorbent, is required an initial activation that may be achieved in different ways. In the case of the present experiments, the thermal treatment of ICs has been applied to activate the surface. A porosity system developed differently represents a result of the applied synthesis conditions. It seems that the water presence within the system due to the involved acids dilution has an important role to form large pores volumes.

If total pores volume is taken into account, as shown in Table 1, the same correspondence with sorption capacity has been noticed, as it was expected, in accordance with the previous discussed correlation.

By means of thermal activation, an intensification of amorphous state of sorbent occurs in detriment of crystalline one, which allows explaining the adsorption

phenomenon not only from kinetic but also from thermodynamic viewpoint, because it is well known that amorphous state is energetically richer than crystalline one. To support this, it has been tried to connect sorption capacity and crystallinity of the expanded specimens. Thus, variation ratio of sorption capacity for specimens E2:E1:E4 is of 4:2.5:1 and variation ratio of the same specimens crystallinity degree is of 1:2.3:4.95.

Characterization of expanded graphite samples after oil sorption by thermal analysis methods

The structural differences between expanded GICs and graphite oxide soot were also reflected in the thermal beaviour of the oil-expanded samples systems that were investigated by thermal analysis methods.

Figure 7 shows the TG, DTA and DTG curves obtained for E4-oil sample; similar thermograms are obtained for all investigated samples. The obtained DTG and DTA curves are presented in comparison in Figs 8–11.

In the temperature range 20–300°C, for each oil-expanded sample, a single step was put in evidence in TG curve. The onset temperature of this process was 150°C. Thus the measured mass cannot be attributed to desorption of some previously adsorbed water because such a process begins at a temperature lower than 150°C. On the other hand, it is well known that the oxidation of pure carbon with O_2 from air does not take place in this temperature range. Each expanded graphite sample was subjected to a thermal analysis in air. Oxidation takes place starting with 700°C or even 800°C. Thus the process could not be related to the graphite conversion to CO_2. Consequently, the process evidenced in TG, DTG and DTA curves consists in the oil oxidation/decomposition with formation of gaseous compounds.

TG curves exhibit a single step and DTG curves show complex shapes (asymmetric shapes, two or three shoulders). It can be noticed that the DTG curve for pristine graphite is placed under the DTG curves of the EG samples. This means that the oxidation rates for oil from the EG samples are substantially higher than the corresponding rates for the pristine graphite. Except the DTA curve for pristine graphite, the DTA curves obtained for the EG samples exhibit complex shapes.

Table 2 lists the main characteristic parameters of the non-isothermal degradation of the investigated samples.

As it can be seen from Figs 8–10 each expanded graphite – oil system has a different thermal behavior. The oxidation rate of the sorbed oil in expanded graphite matrix depends on structural characteristics of the matrix, mainly on the pore type. This is revealed by the displacement of maximum peaks onto DTG curves.

Thus, it is considered that the various structural characteristics of the expanded graphite could be

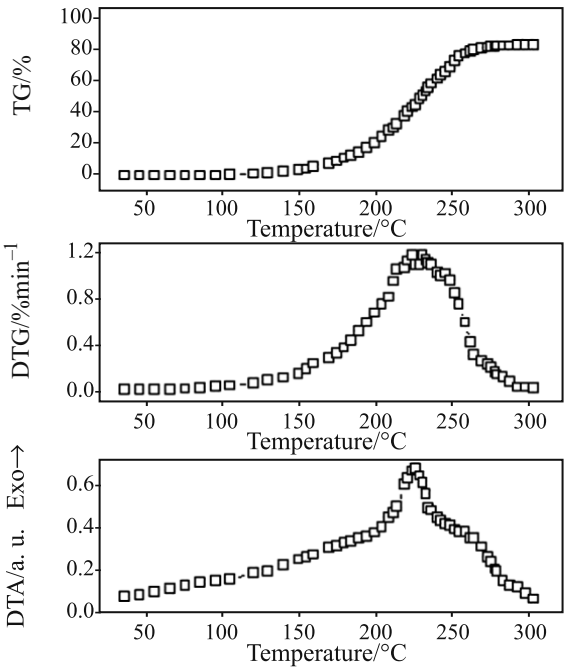

Fig.7 TG, DTG and DTA curves obtained for oxidative removing of oil from E4 system

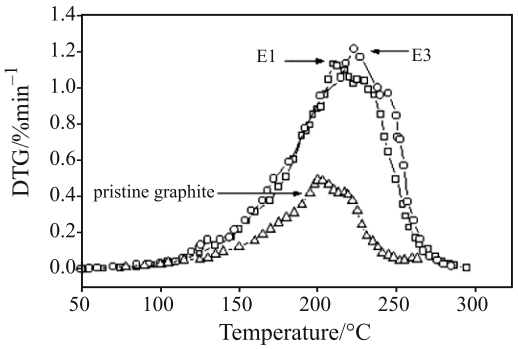

Fig. 8 DTG curves corresponding to expanded E1-oil and E3-oil system

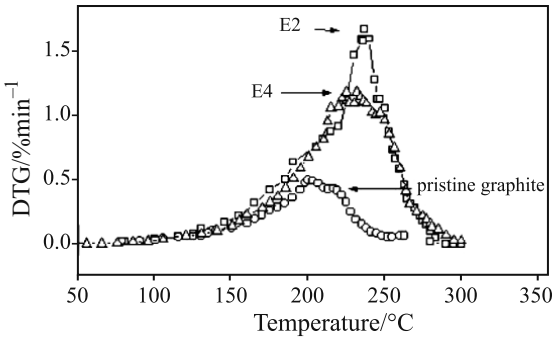

Fig. 9 DTG curves corresponding to expanded E4-oil and E2-oil system

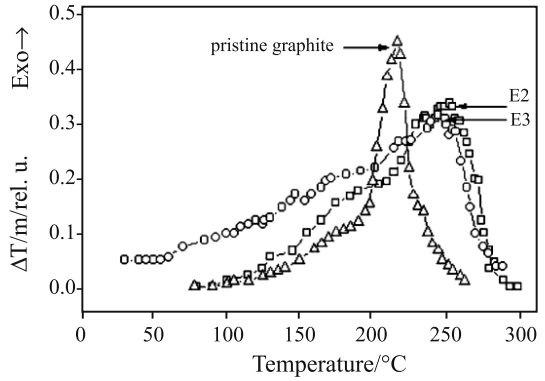

Fig. 10 DTA curves corresponding to expanded E2-oil and E3-oil systems

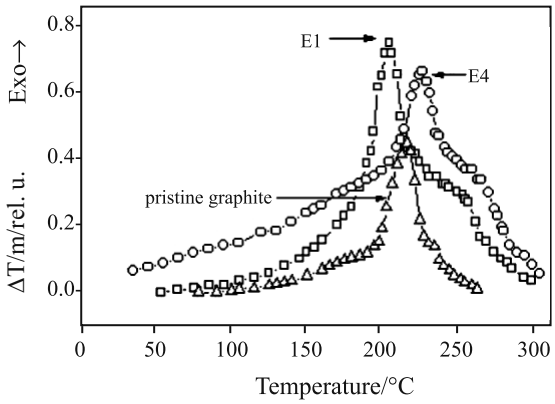

Fig. 11 DTA curves corresponding to expanded E1-oil and E4-oil systems

characterized by means of thermal effect recorded during oil degradation.

Based on thermal analysis experimental result showed in Table 2, it could be observed that:

$$T_{max}^{DTG} \neq T_{max}^{DTA} \quad (1)$$

Table 2 The main characteristics of non-isothermal thermo-oxidative treatment of investigated expanded samples–oil systems

Sample	T_{max} DTG/°C	T_{max} DTA/°C	Δm%	f
E1	210	205	78.8	0.80
E2	237	253	81.7	0.83
E3	223	245	84.2	0.85
E4	225	227	83.9	0.88
Pristine graphite (Natural graphite used as raw material)	200	217	31.7	0.71

T_{max} DTG – the corresponding temperature of the main maximum of DTG curve, T_{max} DTA – the corresponding temperature of the main maximum of DTG curve, Δm% – the total mass loss, f – the ratio between the mass of the removed oil and the mass of the adsorbed oil

$$f<1. \quad (2)$$

The difference between T_{max}^{DTG} and T_{max}^{DTA} could be explained by the mass and the heat transfer phenomena, due to the relative high mass of the samples (≈90 mg). The calculated f values show that the oxidative process is not complete and consequently an amount of ash remains in, or on the surface of the sample. The maximum amount of ash, of 29% from the absorbed oil, resulted in the case of pristine graphite.

Conclusions

- The preparation regime has a significant influence on the characteristics of expanded graphite (EG) and has been evidenced through X-ray diffraction analysis, surface area measurements, bulk densities and oil sorption capacity.
- All investigated EG and graphite oxide soot materials exhibit a rapid and selective absorption of oil from oil-water mixtures.
- Compared to pristine graphite used as raw material and other solid adsorbents, EG prepared materials exhibit a high oil sorption capacity.
- There have been established several empirical correlation between sorption capacity and surface area, bulk density and as well as crystallinity of investigated expanded samples, that showed well defined linear proportionality.

The structural differences among the investigated EG types and graphite oxide soot determines some differences in their thermal behaviors that were put in evidence by means of the thermal analysis methods (TG, DTG and DTA). Thus, it can be mentioned that: a) the thermal effects evolved during non-isothermal heating depend on and reflect the material structure (particularities of a thermal degradation processes of an oil incorporated in an exfoliated graphite matrix, such as: rate of degradation, maximum temperature, thermal effect area etc., could give as some information regarding the type of porosity, related to the rate of oil degradation). In these circumstances thermal analysis method could provide information about the expanded graphite pore system related to sorbed oil oxidation rate.

With this in view, further investigations are in demand to get more information on the relationship between structural parameters of EG materials and functional properties.

References

1 E. Illeková and K. Csomorová, J. Therm. Anal. Cal., 80 (2005) 103.

2 F. Suárez-García, J. Nauroy, A. Martínez-Alonso and J. M. D. Tascón, J. Therm. Anal. Cal., 79 (2005) 525.
3 S. Villar-Rodil, A. Martínez-Alonso and J. M. D. Tascón, J. Therm. Anal. Cal., 79 (2005) 529.
4 Z. Kónya, T. Kanyó, A. Hancz and I. Kiricsi, J. Therm. Anal. Cal., 79 (2005) 567.
5 A. Miyake 1, S. Ando, T. Ogawa and Y. Iizuka, J. Therm. Anal. Cal., 80 (2005) 519.
6 A. W. Atkinson, UK Patents 2149769A, (1983).
7 I. Maryasin, E. Sandbank and G. Shelef, EP patents 0435766, (1999).
8 M. Toyoda, K. Moriya and M Inagaki, Extended abstracts, Eurocarbon 2000, Berlin Germany, (2000) 697.
9 M. A. Savoskin, A. P.Yaroshenko, V. I. Shologon, L. M Kapkan, S. B. Lybchik and O. B. Savsunenko, Extended abstracts, Eurocarbon 2000, Berlin, Germany, (2000) 673.
10 S. Challet, P. Azais, R. J-M. Pelleng, O. Isnard, J.-L. Soubeyrouxand and L. Duclax, J. Phys. Chem. Solids, 65 (2004) 541.
11 K. Jurewicz, C. Vix-Guterl, E. Frackowiac, S. Saadhallah, M. Reda, J. Parmantier, J. Patarin and F. Beguin, J. Phys. Chem. Solids, 65 (2004) 287.
12 Y. Nishi, N. Iwashita, Y. Sawada and M. Inagaki, Water Res. Dec., 36 (2002) 5029.
13 J. Parmentier, S. Saadhallah, M. Reda, P. Gibot, M. Roux, L.Vidal, C. Vix-Guterl and J. Patarin, J. Phys. Chem. Solids, 65 (2004) 139.
14 L. Vovchenco, L. Matzui, M. Zacharenko, M. Babich and A. Brusilovets, J. Phys. Chem. Solids, 65 (2004)171.
15 Ljubisa, R. Radovic and F. Rodriguez-Reinoso, Eds, Chemistry and Physics of Carbon, Marcel Dekker, New York, 1997, Vol. 25, p. 243.
16 M. Inagaki, New Carbons. Control of Structure and Functions, Elsevier Science, Netherland, 2000, p. 147.
17 G. Hristea, Ph.D. thesis, Politechnica University, Bucharest, Industrial Chemistry Faculty, Romania (2001).
18 H. Shioyama, Synth. Met., 114 (2000) 1.
19 Standard: 8432-79: Metallic powders. Bulk density determination. The standard corresponds in part to ISO 3923-1977.
20 F. Rodriguez-Reinoso, M. Molina-Sabio, Adv. Colloid Interface Sci., 76 (1998) 271.
21 P. Harold, A. Klug and E. Leroy, X-ray diffraction procedures polycrystalline and amorphous materials, John Wiley and Sons Inc., 1954, p. 621.
22 M. L. Pyatkovsky, V. M. Ogurko and Yu. I. Semenstrov, Eurocarbon 2000, Berlin, Germany, (2000) 781.
23 T. Nakajima and Y. Matsuo, Carbon, 32 (1994) 469.
24 F. Kay, Y. Leng and T-Y. Zhang, Carbon, 35 (1997) 1089.
25 M. Toyoda and M. Inagaki, Carbon, 38 (2000) 199.

Received: December 15, 2006
Accepted: September 18, 2007

DOI: 10.1007/s10973-006-7465-x